Journal of Visualization, Vol. 8, No. 4 (2005)315-322

Visualizing Görtler Vortices

Winoto, S. H.*, Mitsudharmadi, H.* and Shah, D. A.*

* Department of Mechanical Engineering, National University of Singapore, 10 Kent Ridge Crescent, Singapore 119260, Singapore. E-mail : mpewinot@nus.edu.sg

Received 29 December 2004
Revised 21 June 2005

Abstract : The development of Görtler vortices with pre-set wavelength of 15 mm has been visualized in the boundary-layer on a concave surface of 2.0 m radius of curvature at a free-stream velocity of 3.0 m/s. The wavelength of vortices was pre-set by vertical wires of 0.2 mm diameter located 10 mm upstream of the concave surface leading edge. The velocity contours in the cross-sectional planes at several streamwise locations show the growth and breakdown of the vortices. Three different regions can be identified based on different growth rate of the vortices. The occurrence of a secondary instability mode is indicated by the formation of a small horseshoe eddies generated between the two neighboring vortices traveling streamwise, to form mushroom-like structures as a consequence of the non-linear growth of the Görtler vortices.

Keywords : Görtler vortices, Pre-set wavelength, Mushroom-like structures, Horseshoe vortices, Boundary layer.

1. Introduction

Görtler vortices (Görtler, 1940) are streamwise counter-rotating vortices that may develop in a laminar boundary layer along concave surface, as sketched in Fig. 1. Such vortices are due to centrifugal instability which causes an imbalance between centrifugal force and radial pressure gradient in boundary-layer flow over a concave surface, and will occur if the Görtler number G_θ, as defined by (Smith, 1955):

$$G_\theta = \left(U_\infty \theta / \nu\right) \sqrt{\theta / R} \tag{1}$$

exceeds a critical value $G_{\theta cr}$, where ν is the fluid kinematic viscosity, θ the momentum thickness based on Blasius boundary-layer profile, U_∞ the free-stream velocity, and R the concave surface radius of curvature. The vortices will be amplified downstream resulting in a three-dimensional boundary-layer due to distribution of streamwise momentum which causes spanwise variation in the boundary-layer thickness, and consequently will form the “upwash” region, where low momentum fluid moves away from the wall, and the “downwash” region, where high speed outer fluid moves towards the wall (Fig. 1). At the “upwash”, the boundary-layer is thicker and the shear stress is lower than those at the “downwash”.

Due to the importance of concave surfaces in many fluid engineering applications, such as turbine blades and aerofoils, the effects of Görtler vortices on boundary layer development, heat transfer and deposition, can not be ignored. The wavelength selection of Görtler vortices is not clearly understood yet.

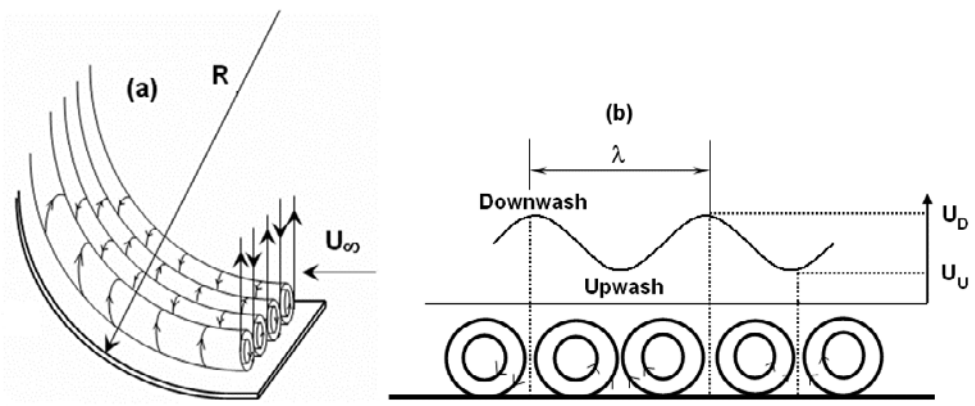

Fig. 1. Sketch of Görtler vortices: (a) flow pattern on concave surface; (b) spanwise distribution of mean streamwise velocity U_∞ showing the definitions of vortex wavelength λ, downwash and upwash.

However, it is known that the onset and development of Görtler vortices are influenced by the initial disturbances, and that the leading edge receptivity influences the resulting vortex wavelengths that appear in the experiments. That is, Görtler instability amplifies the wavelength imposed by the rig on the incoming flow (Kottke, 1988), and a competition of perturbation with different amplification rates, as the only wavelength selection mechanism of Görtler vortices, resulting in non-uniform wavelengths in naturally developing Görtler vortices. Swearingen and Blackwelder (1986) used spectral analysis to determine the vortex wavelength. It gave the same estimation as the average wavelength estimated from the smoke wire visualization of naturally developed Görtler vortices.

By assuming that only vortices with maximum local amplification can appear in the experiments, a simple method based on the Görtler vortex stability diagram (of Smith (1955), for example) can be used to predict the wavelength of Görtler vortices. In this method, the non-dimensional wavelength parameter Λ is defined as:

$$\Lambda = \left(U_\infty \lambda/\nu\right)\sqrt{\lambda/R} \tag{2}$$

where λ is the Görtler vortex wavelength receiving maximum amplification and Λ represents a family of straight lines which cross the Görtler vortex stability diagram (see Mitsudharmadi et al., 2004, for example), αθ is called dimensionless wave number and $\alpha = 2\pi/\lambda$. Luchini and Bottaro (1998) found that the most amplified wavelengths are for Λ ranging from 220 to 270, which agrees with those reported earlier, for example, by Floryan (1991), Smith (1955), and Meksyn (1950) who respectively proposed Λ = 210, 272, and 227.

Visualizations of Görtler vortices can be classified into three groups: 1) Surface flow visualizations, such as those by Highnett and Gibson (1963), McCormack et al. (1970), and Kemp (1977); 2) Suspended particle flow visualizations, such as those by Kahawita and Meroney (1977), Ito (1987), Swearingen and Blackwelder (1987), Petitjeans et al. (1997), and Ajakh et al. (1999); and 3) Electrolytic flow visualizations, such as those by Wortmann (1969), Bippes and Görtler (1972), and Winoto and Crane (1980).

Since the wavelengths of naturally developed Görtler vortices are not uniform, Perhossaini and Bahri (1998) used a series of 0.2 mm-diameter vertical wires placed upstream to concave surface leading edge to pre-set the spanwise position of Görtler vortices. Using this arrangement, the wavelengths of the resulting Görtler vortices are uniform and equal to the spanwise distance of the vertical wires.

The aim of this work is to study the development of Görtler vortices in the boundary-layer on a concave surface of 2.0 m radius of curvature by means of hot-wire anemometry. For convenience and ease of investigation, uniform wavelength Görtler vortices are used. The vortex structures will then be visualized by plotting the contours of streamwise velocity component.

2. Details of Experiment

The experiment was conducted in a curved plexiglas test section of 60^o bend connected to a low speed, blow down wind tunnel. A smooth concave test surface of R = 2.0 m is mounted inside the curved test section at 0.05 m from its bottom surface (Fig. 2). The test section has a rectangular (0.15 m x 0.60 m) cross-section. 13 vertical wires of 0.2 mm diameter are positioned at 10 mm in front of the concave surface leading edge. Since the most amplified wavelength of Görtler vortices can be predicted using Görtler vortex stability diagram by setting the value of Λ in the range of 200 – 270, the present study is conducted by setting the spanwise distance between the vertical wires at 15 mm for U_∞ = 3 m/s, so that Λ = 249. The free stream turbulence level in the test section is about 0.35 % for U_∞ ranging from 1.0 m/s to 6.0 m/s. The von Kárman vortex streets generated behind the wires do not penetrate the boundary-layer, and thus do not affect the generation of Görtler vortices.

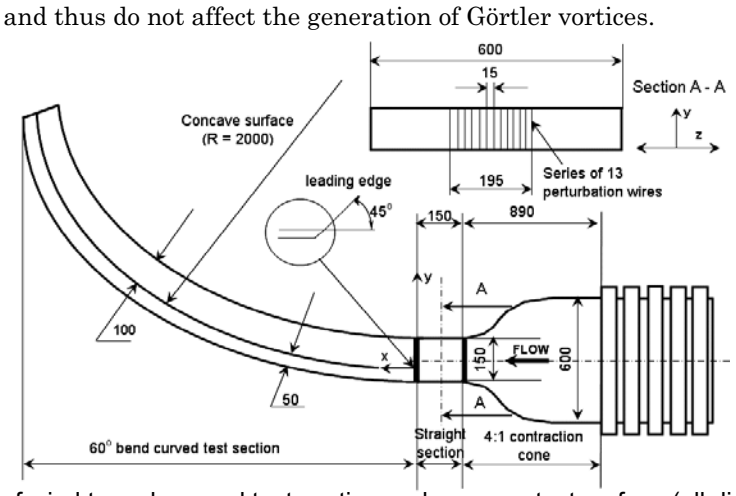

Fig. 2. Sketch of wind tunnel, curved test section and concave test surface (all dimension are in mm).

A single hot-wire probe was used to traverse along a spanwise distance of 60 mm to obtain the mean and fluctuating streamwise velocity component values. The probe was operated in a Constant Temperature Anemometer (CTA) mode, which was coupled to a signal conditioner. The signal was low passed filtered at 3000 Hz and sampled at 6000 Hz for 21 seconds. The data collected were digitized using an analog to digital converter card installed in a personal computer, and were further analyzed using the HPVEE (Hewlett Packard graphical programming) software with operator interface.

A pressure transducer that had been calibrated against a micro-manometer was used in conjunction with a Pitot-static tube that was placed in the free-stream region for the hot-wire calibration. During velocity measurements, the Pitot-static tube was placed in the free-stream region, to monitor the local free-stream velocity. At the end of data acquisition, the probe was placed in the free-stream region and the calibration was re-checked. A more than 2% drift for the sensor was not acceptable and the data would be rejected, resulting in the calibration and data acquisition process to be repeated.

The hot-wire probe and Pitot-static tube were mounted on a traversing mechanism. Two stepper motors controlled the movement of the traversing mechanism along the normal (y) and spanwise (z) directions with an accuracy of ± 0.01 mm. Measurements in the y-z plane were done with the step size of 1.0 mm along the z-direction, while along the y-direction the step size was 0.5 – 1.0 mm depending on the boundary-layer thickness at the measurement station.

3. Results and Discussion

The U/U_∞ contours of in the cross-sectional (y-z) plane at some streamwise (x) locations (Fig. 3) are plotted from the data using a commercially available software called “Tecplot”. To reduce "noise" and minimize discontinuities, the data were smoothened based on the assumption that the second derivative normal to the boundary is constant. To give the effect of rounding off peaks and valleys

rather than eliminating them, 5 points are chosen to be the number of smoothing passes to perform with the relaxation factor for each pass of smoothing is 0.5. Each pass of smoothing shifts the value of a variable at a data point towards an average of the values at its neighboring data points. Smoothing can also be used after inverse-distance interpolation to reduce the artificial peaks and plateaus. For comparison, the mean velocity contours as shown in Fig. 3 have also been plotted using the raw data as reported by Mitsudharmadi et al. (2003).

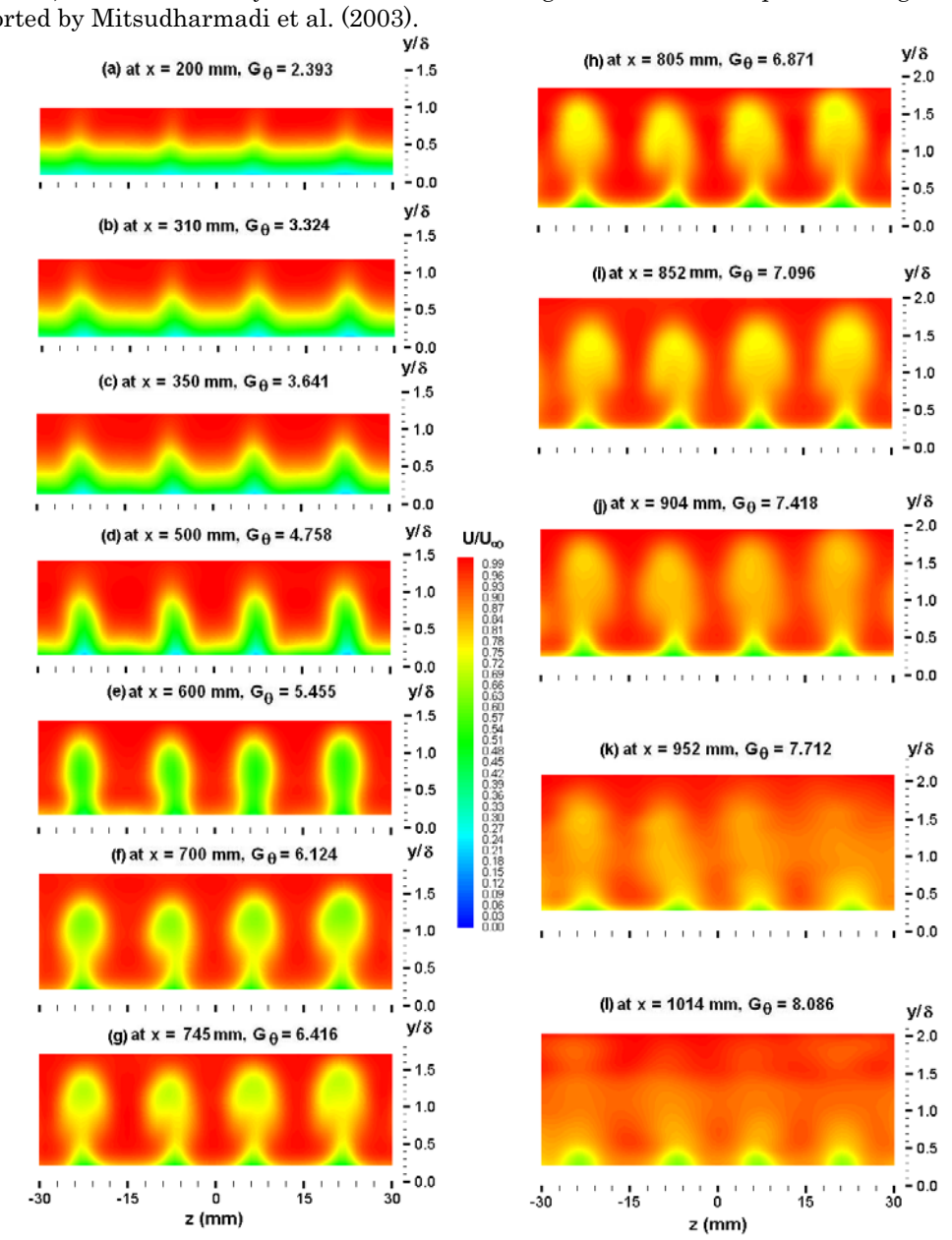

Fig. 3. Mean velocity (U/U_∞) contours showing the evolution of Görtler vortices of pre-set wavelength of 15 mm in boundary layer flow on concave surface of 2.0 m radius of curvature at free-stream velocity U_∞ = 3 m/s. (Note: δ is the Blasius boundary layer thickness).

At x = 200 mm (Fig. 3(a)), the contours are wavy in the spanwise direction, indicating the occurrence of Görtler vortices at this location where G_θ = 2.393. The waviness becomes more pronounced as the flow developed downstream indicating amplification of the vortices, for example, at x = 500 mm (Fig. 3(d)) and when transformed into horseshoe vortices at x = 600 mm (Fig. 3(e)). The transformation of the horseshoe vortices that propagate downstream into mushroom-like structure

before breaking down, is the consequence of the non-linear growth of Görtler vortices (Lee and Liu, 1992). It shows the occurrence of the varicose mode instability as a secondary instability. The mushroom-like vortices as the spanwise structure are clearly shown starting at x = 700 mm (Fig. 3(f)) until x = 852 mm (Fig. 3(i)), after which a decaying process starts from x = 904 mm (Fig. 3 (j)) onwards. The breakdown of the spanwise structure could be attributed to the increase of mixing due to the onset of turbulence. The mushroom-like structures shown in Figs. 3(f) – (j), reveal the structure of finite amplitude Görtler vortices, and the streamwise region in which the mushroom-like structures are coherent and dominating the flow.

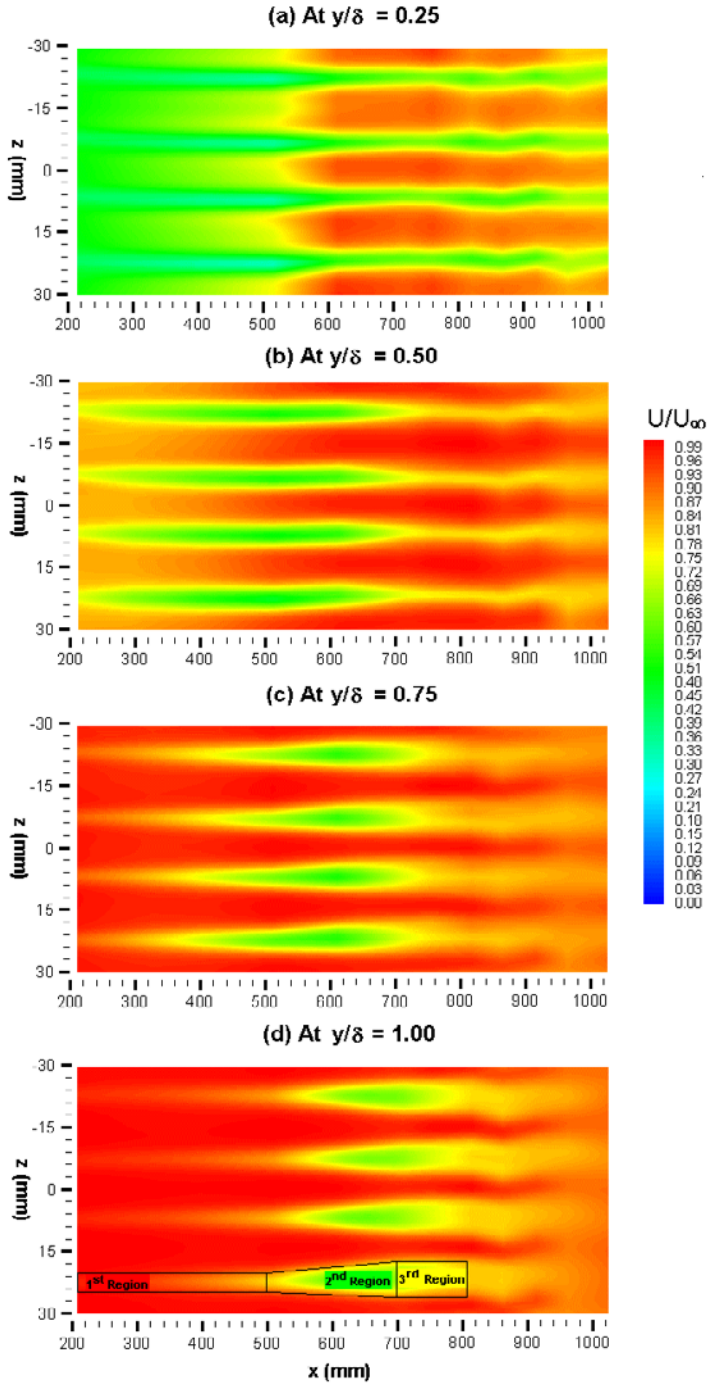

Fig. 4. Mean velocity (U/U_∞) contours in the x-z plane. (Note: δ is the Blasius boundary layer thickness).

The development of the mushroom-like structure is caused by the strong non-linearities in the cross-sectional y-z plane (Lee and Liu, 1992). Close to the "stem" of the mushroom, low momentum fluid is ejected from the wall and returns back toward the wall in the region of maximum shear that results in the shape of mushroom hat.

The contours of U/U_∞ in the x-z plane presented in Fig. 4, show the formation of the streaks of low velocity (upwash) regions. The high velocity (downwash) regions occur in the spacing between the wires at which the boundary-layer thickness is thinner than that in the low velocity (upwash) regions that occur downstream of each vertical wire. These agree with Perhossaini and Bahri (1998) who carried out the experiment for G_θ ranging from 2 to 7.7 at U_∞ = 2.0 m/s, wire spacing of 30 mm and R = 0.65 m.

As indicated in Fig. 4(d) and Fig. 5, three different regions can be identified based on the growth rate of Görtler vortices in term of the maximum disturbance amplitude as defined by Eqn. (3). Since the smaller growth is initiated at the location where the inflection point is observed in the boundary-layer velocity profile at x = 500 mm, and the formation of the inflection point in the velocity profile is also an indicator to predict the onset of non-linear region. Hence, referring to Fig. 4(d), the 2nd and 3rd regions are considered as the non-linear region in which the primary disturbance grows at a smaller rate than in the 1st or linear region (see Mitsudharmadi et al., 2004).

In the 1st region, the width of the low speed streaks increases more gradually (until $x \approx 500$ mm), compared to growth of the low speed streaks in the 2nd region (see Fig. 4(d)). The difference in the width growth rate of the low speed streaks could be due to the transformation from the wavy shape into the horseshoe vortices that propagate downstream to form the mushroom-like structures. This transformation is observed at $x \approx 500$ mm as shown in Fig. 3(d). The width of the low speed streaks is invariant in the 3rd region indicating finite amplitude of the disturbances. By examining the phenomena presented in Figs. 3(a) – (l), it is found that the 3rd region (Fig. 4(d)) coincides with the region in which the mushroom-like structures are dominant in the boundary-layer flow (Figs. 3 (f) – (h)). This region is followed by the meandering of the vortices, that is, the side way oscillation of the low speed streaks which take place at x of around 800 mm, as depicted in Figs. 4(a) – (d). This phenomenon indicates the presence of the secondary instability mode called sinuous mode that is believed to lead the flow to turbulence (Bakchinov et al., 1995). Accordingly, the 1st region can be attributed to the linear growth of the Görtler vortices.

The streamwise disturbance amplitude that is defined as:

$$\kappa_u(\eta) = \left\{ U_D(\eta) - U_U(\eta) \right\} / 2U_\infty \qquad (3)$$

where U_D is the mean velocity at downwash, U_U the mean velocity at upwash and $\eta = \sqrt{(U_\infty / x\,\nu)}$ represents the dimensionless coordinate normal to the wall, was also used by Finnis and Brown (1989) to determine the maximum disturbance amplitude (κ_{umax}) at every streamwise (x) location. The streamwise variation of κ_{umax} is presented in Fig. 5. Comparing with the phenomenon depicted in Fig. 4(d), it is shown that κ_{umax} in the 2nd and 3rd region that coincides with nonlinear region in Fig. 5, increases exponentially with growth rate lower than that in the 1st region. This could be attributed to the occurrence of the 3rd region in which the finite amplitude of the disturbance is reached and the flow is dominated by the mushroom-like structure. This region is followed by the region where κ_{umax} decreases exponentially showing the saturation of the disturbance amplitude after the disturbance finite amplitude has been reached. This agrees with Schmid and Henningson (2001) who found that once the disturbance has reached a finite amplitude at which the boundary-layer flow is dominated by the mushroom-like structures, it often saturates and transforms the flow into a new possibly steady state in which secondary instabilities can grow. However, the spectrum analysis of the fluctuating component u′ shows that the secondary instabilities arise prior to the non-linear saturation as exhibited by the formation of the peak in the spectrum with a band between 50 to 200 Hz at the streamwise location, where the amplitude of the disturbance is still developing (Mitsudharmadi et al., 2005).

Another indicator to predict the location of the start of the non-linear region is the formation of an inflection point in the boundary-layer velocity profile at the upwash. The horseshoe vortices as the secondary instability of Görtler vortices are known to be caused by the high shear layer formed near the boundary-layer edge (Floryan, 1991). This high shear layer is a consequence of the formation of the inflection point in the velocity profile which is initially detected at the streamwise location $x \approx 500$ mm (Mitsudharmadi et al., 2004).

The larger amplitude of the disturbances in the non-linear region (Fig. 5) will lead to point of inflection in the upwash velocity profiles (Mitsudharmadi et al., 2004), as also reported by Wortmann (1969), Aihara and Koyama (1981), and Swearingen and Blackwelder (1987). In the non-linear growth region (x = 500 – 852 mm), the spanwise variations of the mean streamwise velocity become flattened at the downwash (high velocity) locations, and narrow and sharp at the upwash (low velocity) locations as shown by Aihara and Koyama (1981) and recently by Mitsudharmadi et al. (2004).

The formation of high shear layer near the edge of the boundary-layer causes the formation of the second peak near the edge of boundary-layer in the turbulence intensity profile at the upwash which starts at x = 500 mm (Mitsudharmadi et al., 2004). This initiates the development of the horseshoe vortices as the secondary instability(Floryan, 1991). As the horseshoe vortices

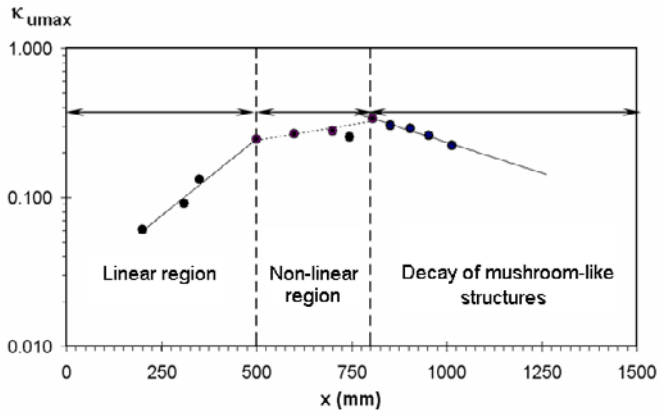

Fig. 5. Distribution of maximum disturbance amplitude showing the linear and non-linear (exponential) growth of vortices in the boundary-layer flow on concave surface of 2.0 m radius of curvature at U_∞ = 3 m/s.

propagate downstream and breakdown, the turbulence spreads out in the boundary-layer resulting in the decay of the second peak near the boundary-layer edge until the turbulence near the wall become dominant in the flow. The decay process of the second peak is related to the breakdown of vortex structure in the boundary-layer flow prior to turbulence.

4. Conclusion

Using the velocity data obtained from hot-wire anemometer measurement, the flow field of Görtler vortices with pre-set wavelength has been visualized, prior to turbulence. The amplification of the vortices will continue until $G_\theta = G_{\theta tr}$ is reached where the start of boundary-layer transition occurs (see Mitsudharmadi et al., 2004, for the details). This study of pre-set wavelength Görtler vortices has provided more information on the development stages of such vortices. The pre-set vortex wavelength is found to be equal to the spanwise spacing of the vertical wires until the streamwise location where the vortices breakdown prior to turbulence.

The velocity contours in the x-z as well as in y-z planes show that the spanwise modulation of streamwise velocity U is equal to the 15 mm spanwise spacing of the vertical wires. The velocity contours in the y-z plane show the non-linear region of the vortices in which the boundary-layer flow is dominated by the mushroom-like structures that have reached finite amplitude. This region is followed by meandering of the vortices which indicates the presence of sinuous mode instability that evolves rapidly to lead the flow to turbulence.

References

Aihara, Y. and Koyama, H., Secondary instability of Görtler vortices-formation of periodic three-dimensional coherent structure, Trans. Japan Soc. Aero. Space. Sci., 24-64 (1981), 78-94.

Ajakh, A., Kestoras, M. D., Toe, R. and Perhossaini, H., Influence of forced perturbation in the stagnation region on Görtler instability, AIAA Journal, 37-12 (1999), 1572-1577.

Bippes, H. and Görtler, H., Dreidimensionale Störungen in der Grenzschicht an einer konkaven Wand, Acta Mechanica, 14-4 (1972), 251.

Finnis, M. V. and Brown, A., Stability of a laminar boundary-layer flowing along a concave surface, Journal of Turbomachinery Transaction of the ASME, 111-4 (1989), 376-386.
Floryan, J. M., On the Görtler instability of boundary-layer, Progress in Aerospace Science, 28 (1991), 235-271.
Görtler, H., Über eine dreidimensionale Instabilität laminarer Grenzschichten an konkaven Wänden, Ges. D. Wiss. Göttingen, Nachr. a. d., Math., 2-1 (1940); translated as "On the three-dimensional instability of laminar boundary layers on concave walls", NACA TM 1375 (1954).
Highnett, E. T. and Gibson, M. M., Surface flow patterns as visualized by dust deposits on the blades of a fan, J. Roy. Aeronaut. Soc., 67 (1963), 589.
Ito, A., Visualization of boundary layer transition along a concave wall, Proceedings of the 4th International Symposium on Flow Visualization (Paris), (1987), 339-344.
Kahawita, R. A. and Meroney, R. N., The influence of heating on the stability of laminar boundary layers along concave curved walls, ASME J. Appl. Mech., 44-1 (1977), 11-17.
Kemp, A. S., The boundary layer on the pressure face of turbine blades in cascade, (1977), Ph. D. Thesis, Cambridge University, England, U. K.
Kottke, V., On the instability of laminar boundary-layer along a concave wall towards Görtler vortices, Propagation and Non Equilibrium Systems, (1988), Springer, Berlin.
Lee, K. and Liu, J. T. C., On the Growth of mushroom-like structures in non-linear spatially developing Görtler vortex flow, Physics of Fluids A., 4-1 (1992), 95-103.
Luchini, P. and Bottaro, A., Görtler vortices: a backward-in-time approach to the receptivity problem, Journal of Fluid Mechanics, 363 (1998), 1-23.
McCormack, P. D., Welker, H. and Kelleher, M., Taylor-Görtler vortices and their effect on heat transfer, ASME J. Heat Transfer, 92-1 (1970), 101-112.
Meksyn, D., Stability of viscous flow over concave cylindrical surfaces, Proc. Roy. Soc., A203 (1950), 253.
Mitsudharmadi, H., Winoto, S. H. and Shah, D. A., Development of Görtler vortex flow with forced wavelength, Proceedings of the 7th Asian Symposium on Visualization (Singapore), (2003), Paper 5A-5.
Mitsudharmadi, H., Winoto, S. H. and Shah, D. A., Development of boundary layer flow in the presence of forced wavelength Görtler vortices, Physics of Fluids, 16-11 (2004), 3983-3996.
Mitsudharmadi, H., Winoto, S. H. and Shah, D. A., Secondary instability in forced wavelength Görtler vortices, Physics of Fluids, 17-7 (2005), 074104-1.
Peerhossaini, H. and Bahri, F., On the spectral distribution of the modes in non-linear Görtler instability, Experimental Thermal and Fluid Science, 16-3 (1998), 195-208.
Petitjeans, P., Aider, J. L. and Weisfreid, J. E., Mass and momentum transport in longitudinal vertical structures in liquid flow. Example of Görtler vortices, Experiments in Fluids, 23 (1997), 388-394.
Schmid, P. J. and Henningson, D. S., Stability and transition in shear flows, Applied Mathematical Sciences, 142 (2001), Springer-Verlag, New York.
Smith, A. M. O., On the growth of Taylor-Görtler vortices along highly concave wall, Quart. Appl. Mech., 13 (1955), 230-262.
Swearingen, J. D. and Blackwelder, R. F., Spacing of the streamwise vortices on concave walls, AIAA Journal, 24-10 (1986), 1706-1709.
Swearingen, J. D. and Blackwelder, R. F., The growth and the breakdown of streamwise vortices in the presences of a wall, Journal of Fluid Mechanics, 182 (1987), 255-290.
Winoto, S. H. and Crane, R. I., Vortex structure in laminar boundary layers on a concave wall, Int. J. Heat and Fluid Flow, 2-4 (1980), 221-231.
Wortmann, F. X., Visualization of transition, Journal of Fluid Mechanics, 38 (1969), 473-480.

Author Profile

S. H. Winoto: He obtained his Ph.D. from Imperial College, London in 1980 and joined the National University of Singapore in the same year. He has been a Visiting Professor at Georgia Institute of Technology and University of Southern California and has been involved in organizing some international meetings in Singapore, such as the 7th Asian Symposium on Visualization, 3 – 7 November 2003. He is a member of the American Society of Mechanical Engineers (ASME), and has been the President/Chairman of the ASME Singapore Chapter/Section and also the Chairman of the Asia-Pacific Zone of ASME Region XIII. His research interests include boundary layer flows, jet flows and their application, flow visualizations and lubrication.

Hatsari Mitsudharmadi: He obtained his Master of Engineering (MEng) degree in Mechanical Engineering from National University of Singapore and currently he is pursuing a Ph.D. program at the Department of Mechanical Engineering in the same university. His research interests are boundary layer flows and hot-wire anemometry.

D. A. Shah: He obtained his Master of Engineering from Indian Institute of Science, Bangalore, India in 1980 and PhD from University of Newcastle, Australia in 1988. He spent about a year as a faculty member at the Indian Institute of Technology, Kanpur, India before joining the National University of Singapore in 1989. He has been involved in organising some international conferences in Singapore. He is a member of the American Society of Mechanical Engineers (ASME) and has served on a number of Committees in the ASME Singapore Section. His research interests include hot-wire anemometry, turbulent shear flows, bluff bodies and industrial aerodynamics.